NUMERICAL ANALYSIS OF ELASTIC CONTACT BETWEEN FOURTH ORDER POLYNOMIAL SURFACES

Dorin Gradinaru, Sergiu Spinu
"Stefan cel Mare" University of Suceava, Romania
gradinaru@fim.usv.ro, sergiu.spinu@fim.usv.ro

Keywords: numerical simulation, elastic contact, polynomial surfaces, contact parameters, stress state

Abstract: The closed-form solution advanced by Diaconescu for elastic contact between fourth order polynomial surfaces is validated in this paper through numerical analysis. Contact parameters (contact area and pressure distribution) are assessed numerically using the well-known algorithm advanced by Polonsky and Keer. Stress state in contacting bodies is computed according to superposition principle and fundamental solutions for the elastic half-space, and spectral methods are applied for acceleration of computation. Stress tensor components, and equivalent von Mises stress on the contact area, at a fixed depth and on the central axis of the contact, are depicted and discussed in detail.

1. INTRODUCTION

Improvement of load-carrying capacity of mechanical contact requires a uniform pressure distribution over contact area. This goal cannot be achieved with quadratic surfaces, as assumed by the Hertz formalism. Therefore, the contact between high order polynomial surfaces should be investigated.

In an extension of Hertz theory, based on the works of Shtaerman, [8], and Galin, [5], Diaconescu, [2], establish the analytical equations governing the contact between high order polynomial surfaces. These relations allow formulation of an improved contact geometry, [3], which guarantees a more uniform pressure distribution on the contact area.

The closed-form solution for the contact between fourth order polynomial surfaces is validated numerically in this paper. Contact analysis is completed by assessing stress state features. To this end, stress tensor components, as well as equivalent von Misses tension, are computed numerically, following a method advanced by Liu, Wang and Liu, [6].

2. OVERVIEW OF EXISTING ANALYTICAL SOLUTION

In an extension of Hertz theory, Diaconescu, [2], advanced a closed-form solution for the elastic contact between bodies bounded by fourth order polynomial surfaces. Using the equivalent contact method, the composite initial contact geometry can be expressed as:

$$hi(x,y) = A \cdot x^4 + B \cdot y^4 + C \cdot x^2 y^2, \tag{1}$$

where A, B and C are parameters, not all independent. Contact half-axes a and b, central pressure p_0, and rigid-body approach δ, result from the following relations:

$$a = n_a \cdot \sqrt[5]{\frac{5\eta Q}{12A}};\ n_a = \sqrt[5]{\frac{(2+e^2)\cdot K(e) - 2\cdot(1+e^2)\cdot E(e)}{\pi \cdot e^4}}; \tag{2}$$

$$b = n_b \cdot \sqrt[5]{\frac{5\eta Q}{12B}};\ n_b = \sqrt[5]{\frac{\sqrt{1-e^2}\left[(3\cdot e^4 - 5\cdot e^2 + 2)\cdot K(e) - 2\cdot(1-2\cdot e^2)\cdot E(e)\right]}{\pi \cdot e^4}}; \tag{3}$$

$$p_0 = \frac{n_p}{\pi} \cdot \sqrt[5]{\frac{125 \cdot A \cdot B \cdot Q^3}{54 \cdot \eta^2}} \; ; \; n_p = \frac{1}{n_a \cdot n_b} ; \tag{4}$$

$$\delta = \frac{n_\delta}{2} \cdot \sqrt[5]{\frac{625}{648} A \eta^4 Q^4} \; ; \; n_\delta = \frac{3 \cdot K(e)}{\pi \cdot n_a} , \tag{5}$$

where Q denotes the statically applied normal force , K and E are the complete elliptic integrals of the first and of the second kind respectively, and η is the elastic constant of the contact. Eccentricity e of contact ellipse result from solving numerically the following transcendental equation:

$$\frac{A}{B} = (1-e^2)^2 \cdot \frac{(2+e^2) \cdot K - 2 \cdot (1+e^2) \cdot E}{(3 \cdot e^4 - 5 \cdot e^2 + 2) \cdot K - 2 \cdot (1-2 \cdot e^2) \cdot E} . \tag{6}$$

Diaconescu, [2], proves that, in order to obtain an elliptical contact area, parameter C must obey the following relation:

$$C = \frac{3 \eta p_0}{e^4 a^2 b} \cdot \left[(2-e^2) \cdot E - 2 \cdot (1-e^2) \cdot K \right], \tag{7}$$

which leads to the following pressure distribution:

$$p(x,y) = p0 \cdot \sqrt{1 - \frac{x^2}{a^2} - \frac{y^2}{b^2}} \cdot \left[1 + 2 \cdot \left(\frac{x^2}{a^2} + \frac{y^2}{b^2} \right) \right]. \tag{8}$$

3. CONTACT PARAMETERS

Results obtained using the analytical model (2) - (8) are compared with numerical predictions of an elastic contact solver based on the conjugate gradient method advanced by Polonsky and Keer, [7]. A detailed description of the program is given elsewhere, [4]. The following input is used in both analytical and numerical approaches: $Q = 1kN$, $A = 1m^{-3}$, $B = 9m^{-3}$. The parameter C computed from Eq. (7) yields $C \approx 5.83 m^{-3}$. The materials of the contacting bodies have the following elastic properties: Young modulus, $E_1 = E_2 = 210\,GPa$, Poisson's ratio, $\nu_1 = \nu_2 = 0.3$.

In figures 1 and 2, depicting the pressure distribution on the contact area and in the plane $y = 0$, dimensionless pressure is defined as ratio to central pressure, $\bar{p} = p / p_0$. A good agreement between analytical and numerical results is found. Relative errors between analytical and numerical sets of contact parameters are depicted in Table 1.

Table 1. Contact parameters and relative errors

	Analytical model	***Numerical model***	***Relative error***
Maximum pressure, [MPa]	1.77142	1.77411	0.1518%
Central pressure p_0, [MPa]	1.26603	1.26368	0.1859%
Contact ellipse major half-axis a, [m]	2.02078e-02	2.02078e-02	0%
Contact ellipse minor half-axis b, [m]	1.04795e-02	1.04795e-02	0%
Rigid body approach δ, [m]	3.62432e-07	3.62323e-07	0.03%

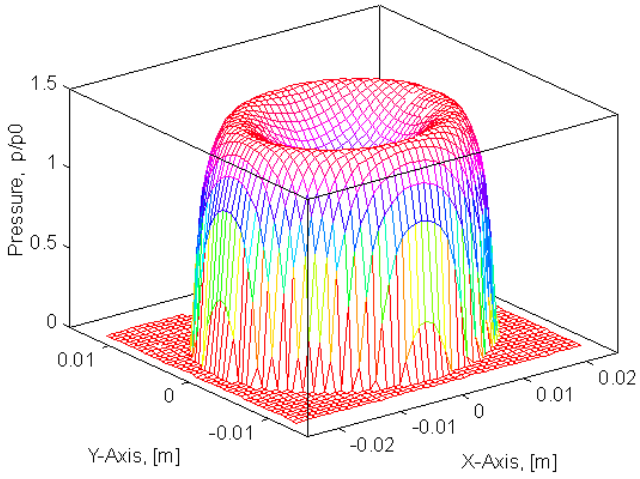

Figure 1. Pressure distribution on elliptic contact area

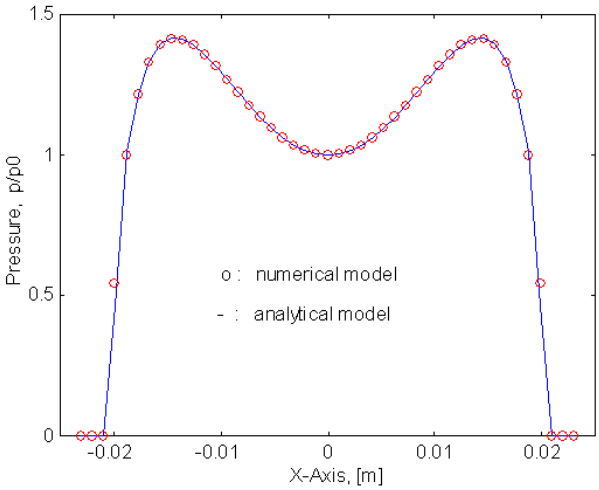

Figure 2. Pressure profile in the plane $y = 0$

4. STRESS STATE COMPUTATION

It is common practice to assimilate the contacting bodies with elastic half-spaces. This assumption holds if the dimensions of contact area are small compared to significant dimensions of contacting bodies, and allows expressing contact stresses according to superposition principle:

$$\sigma_{ij}(x,y,z) = \iint_{\Gamma_C} p(x',y') \cdot G_{ij}\left(x-x',\ y-y',\ z\right)dx'dy', \tag{9}$$

where $G_{ij}\left(x,y,z\right)$ denotes stress components ij induced by a unit force applied in origin, Γ_C is the contact area, and $i,j = x,y,z$. Functions G_{ij}, also referred to as fundamental solutions or Green functions, were derived by Boussinesq, [1]. Integral in Eq. (9) cannot be performed analytically except for a few cases. Its discrete counterpart is the following relation, which, unlike Eq. (9), can be computed numerically for any pressure distribution or contact area:

$$\sigma_{\zeta\xi}(i,j,m) = \sum_{(k,\ell)\in A_C} D_{\zeta\xi}(i-k,j-\ell,m) \cdot p(k,\ell,0), \tag{10}$$

where $D_{\zeta\xi}$ is the so called influence coefficient, expressing the stress component $\zeta\xi$, $\zeta,\xi = x,y,z$, induced in the cell (i,j,m) by a unit pressure acting in the cell (k,ℓ) in the discrete contact area A_C:

$$D_{\zeta\xi}(i-k,j-\ell,m) = \int_{y(\ell)-\Delta_y/2}^{y(\ell)+\Delta_y/2}\ \int_{x(k)-\Delta_x/2}^{x(k)+\Delta_x/2} G_{\zeta\xi}\left(x(i)-x',y(j)-y',z(m)\right)dx'dy', \tag{11}$$

with Δ_1 and Δ_2 the mesh steps along corresponding directions. Influence coefficients in Eq. (10) can be computed using the following relation:

$$D_{\zeta\xi}(i,j,m) = d_{\zeta\xi}(x(i)+\frac{\Delta_x}{2}, y(j)+\frac{\Delta_y}{2}, z(m)) + d_{\zeta\xi}(x(i)-\frac{\Delta_x}{2}, y(j)-\frac{\Delta_y}{2}, z(m))...$$
$$-d_{\zeta\xi}(x(i)+\frac{\Delta_x}{2}, y(j)-\frac{\Delta_y}{2}, z(m)) - d_{\zeta\xi}(x(i)-\frac{\Delta_x}{2}, y(j)+\frac{\Delta_y}{2}, z(m)), \quad (12)$$

with functions $d_{\zeta\xi}$ given in Appendix. The most efficient way to compute the multi-summation in Eq. (10), which is in fact a two-dimensional convolution, is through spectral methods. According to convolution theorem, the convolution of two signals, each having N samples, requires $O(N^2)$ operations in time/space domain, but only $O(N\log N)$ in frequency domain, where it reduces to element-wise product. However, when transferring to frequency domain via Fast Fourier Transform, presumption of signal periodicity is assumed, which leads to contamination of convolution result due to spurious neighboring periods. Liu, Wang and Liu, [6], advanced a fast and robust algorithm to circumvent periodicity error, which is also applied here. This algorithm is able to assess linear convolution by computing the discrete cyclic convolution of the two terms on an extended domain, with a special, "wrapped-around" order of influence coefficients.

5. RESULTS

Two-dimensional distributions of stress components, as well as the equivalent von Mises stress σ_{HMH} on the contact area, are presented in Fig. 3. Dimensionless stresses $\bar{\sigma}$ are defined as ratio to central pressure p_0, $\bar{\sigma} = \sigma / p_0$. The following relation is verified everywhere on the contact area: $\bar{\sigma}_x(i,j) < \bar{\sigma}_y(i,j) < \bar{\sigma}_z(i,j), (i,j) \in A_C$. The maximums of these distributions are: $\bar{\sigma}_x \cong 0.75, \bar{\sigma}_y \cong 0.88, \bar{\sigma}_z \approx 1$. Along contact ellipse axes, normal stress profiles exhibit a local minimum in contact center and two local maximums at the boundary of the contact area. Shear stress τ_{xy} profile displays two maximums and two minimums on the contact boundary, having a modulus equal to $0.12p_0$. The other two shear stresses vanish on the contact area, thus verifying boundary condition. Von Mises equivalent stress reaches its maximum, $\bar{\sigma}_{HMH} = 0.25$, along minor axis of contact ellipse.

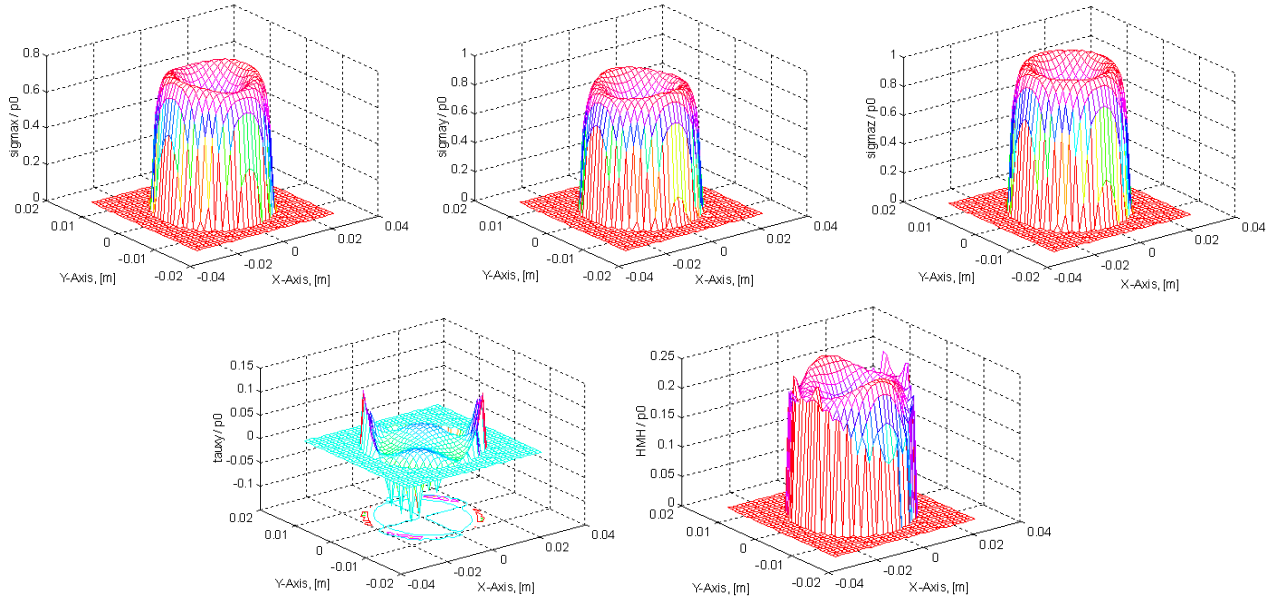

Figure 3. Contact stresses on the contact area

Stress components in the subsurface, in a layer located at depth $z = 0.8b$, are presented in Figure 4.a to f. Distributions of normal stresses along the directions of major and of minor contact ellipse axes are depicted in Figures 5 and 6, respectively. Normal stresses reach their maximums in the center of the contact: $\bar{\sigma}_x = 0.21$, $\bar{\sigma}_y = 0.13$, and exhibit two inflection points along the major and the minor contact ellipse, respectively. Shear stress $\bar{\tau}_{xy}$ vanish along contact ellipse axes and displays two maximums and two minimums, having a modulus of 0.052.

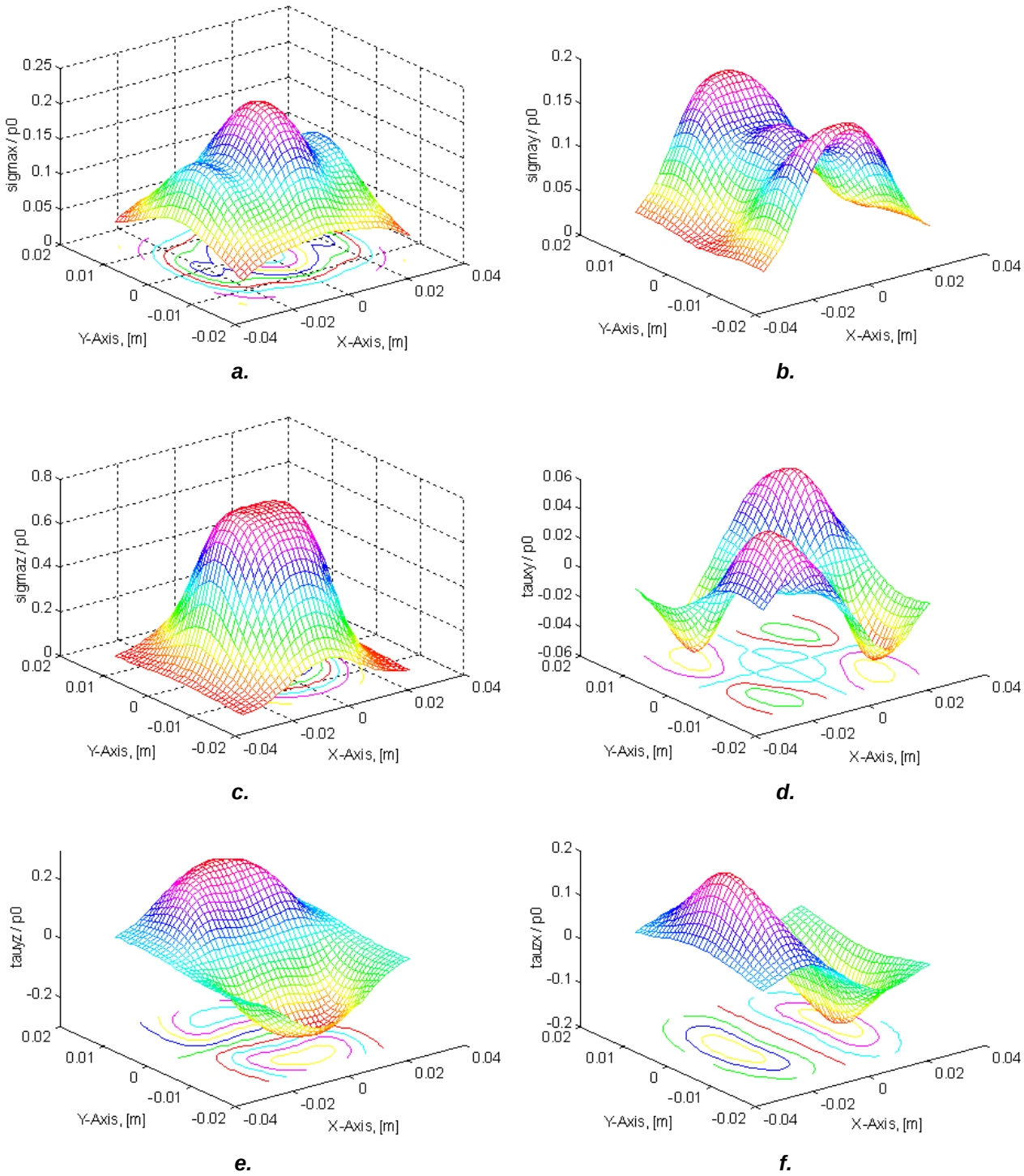

Figure 4. Contact stresses at depth $z = 0.8b$

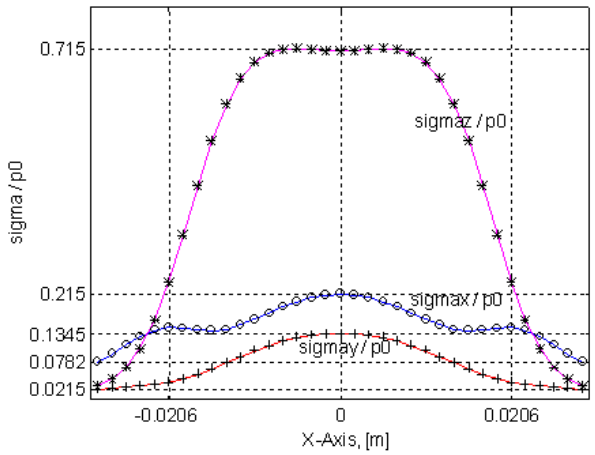

Figure 5. Normal stresses along major axis

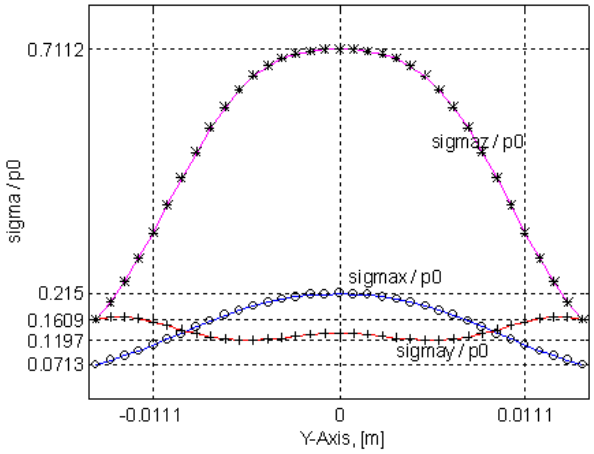

Figure 6. Normal stresses along minor axis

The equivalent von Mises stress on the contact area and along directions of X and Y Axes, are depicted in Figure 7. Its maximum, $\bar{\sigma}_{HMH} = 0.58$, is reached along direction of major axis.

The stress components along central axis of the contact, as well as the maximum principal shear stresses τ_i, $i = 1,2,3$, are depicted in Figure 8. Normal stresses σ_x and σ_y reach their maximums on the surface, and σ_z displays a maximum of $\bar{\sigma}_z = 0.76$ at depth $z = 0.47b$.

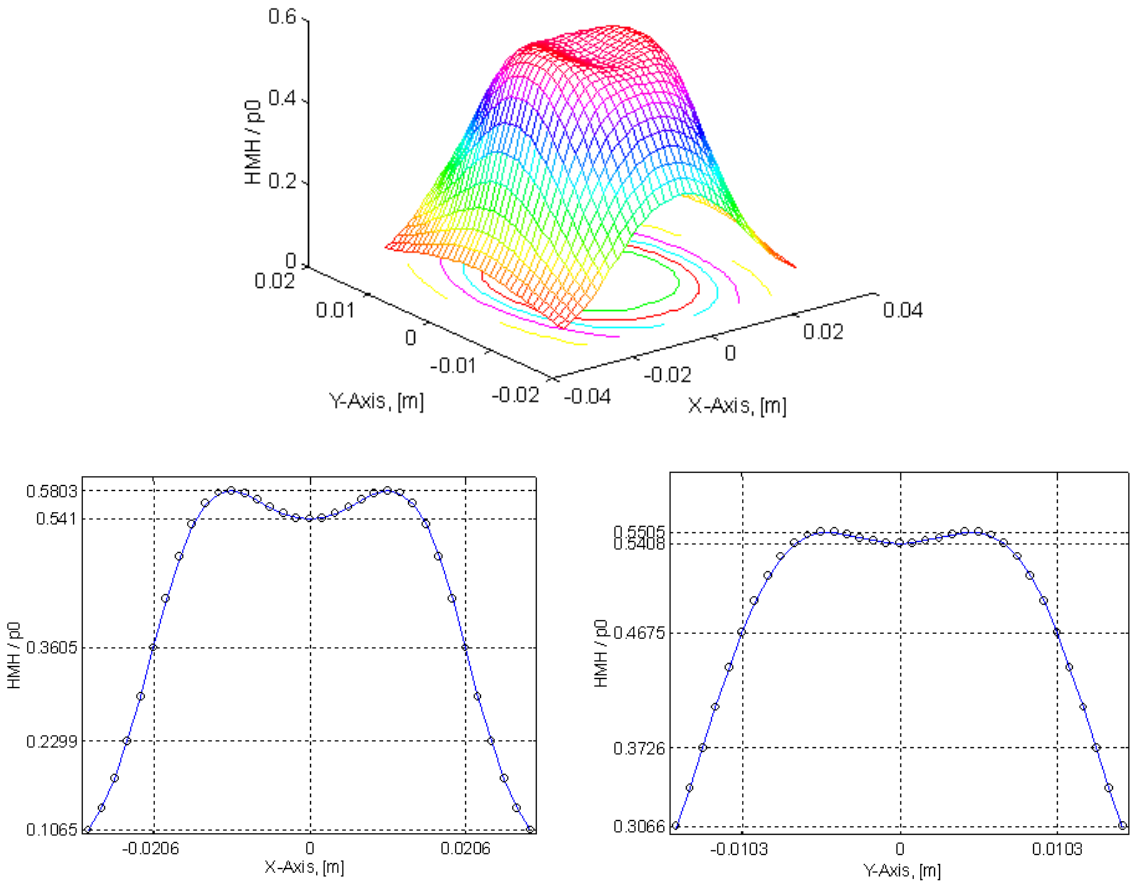

Figure 7. Equivalent von Mises stress at depth $z = 0.8b$

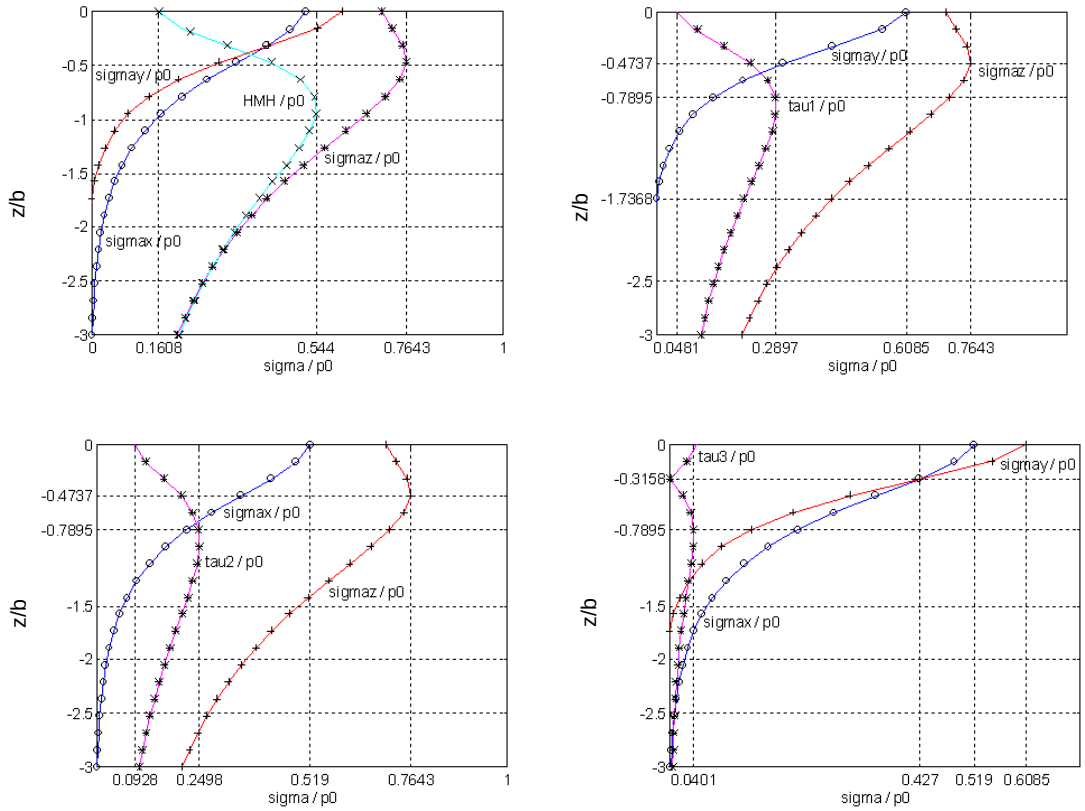

Figure 8. Stress components on the central axis of the contact

6. CONCLUSIONS

The elastic contact between bodies bounded by fourth order polynomial surfaces is investigated numerically in this paper. Contact area and pressure distribution are assessed using the well-known algorithm by Polonsky and Keer. Program predictions match well closed-form solution advanced by Diaconescu for this type of contact geometry and material behavior.

The stress states on the contact area, in subsurface and on the central axis of the contact, are computed using superposition principle and Boussinesq fundamental solutions for a unit normal force acting on half-space boundary. Multi-summation calculation is accelerated by computing the arising convolution products in the frequency domain, where convolution is substituted by element-wise product, according to the technique advanced by Liu, Wang and Liu.

Position of maximums of stress tensor components, as well as of equivalent von Mises stress, are assessed.

References

[1] Boussinesq, J., (1969), Application des potentiels á l'etude de l'equilibre et du mouvement des solides élastiques. Reed. A. Blanchard, Paris.

[2] Diaconescu, E. N., (2003), Hertz Theory Revisited, private communication, Opening Plenary Session of 10th Romanian Tribology Conference, Galati.

[3] Diaconescu, E. N., (2006), Elliptic Elastic Contact between High Order Symmetrical Surfaces, ASME Journal of Tribology, Vol. 128, pp. 908-914.

[4] Frunza, G., Spinu, S., Frunza, M. C., (2009), Numerical Simulation of Pressure Distribution in Multiasperity Dental Contacts, Annals of the University of Oradea, Fascicle of Management and Technological Engineering, CD-ROM Edition, Volume VIII (XVIII), 2009, ISSN 1583-0691.

[5] Galin, L. A., (1953), Contact Problems in the Theory of Elasticity (in Russian), Gostehizdat, Moscow, pp. 206–211.
[6] Liu, S. B., Wang, Q., and Liu, G., (2000), A Versatile Method of Discrete Convolution and FFT (DC-FFT) for Contact Analyses. Wear, 243 (1–2), pp. 101–111.
[7] Polonsky, I. A., and Keer, L. M., (1999), A Numerical Method for Solving Rough Contact Problems Based on the Multi-Level Multi-Summation and Conjugate Gradient Techniques. Wear, 231(2), pp. 206–219.
[8] Shtaerman, I., (1949), Contact Problems in the Theory of Elasticity, (in Russian), Gostehizdat, Moscow.

APPENDIX

The functions d_{ij} needed to compute influence coefficients in Eq. (12) are obtained by integration of Boussinesq fundamental solution over a rectangular patch. The following primitives can be used:

$$d_{xx}(x,y,z)=\frac{1}{2\pi}\left[\frac{xyz}{r(x^2+z^2)}+(1-2\nu)\left(\tan^{-1}\left(\frac{x}{y}\right)-\tan^{-1}\left(\frac{xz}{yr}\right)\right)-\tan^{-1}\left(\frac{xy}{zr}\right)\right]; \quad (13)$$

$$d_{yy}(x,y,z)=d_{xx}(y,x,z); \quad (14)$$

$$d_{zz}(x,y,z)=-\frac{1}{2\pi}\tan^{-1}\left(\frac{xy}{zr}\right)-\frac{xyz(r^2+z^2)}{r(x^2+z^2)(y^2+z^2)}; \quad (15)$$

$$d_{xy}(x,y,z)=\frac{1}{2\pi}\left[(2\nu-1)\log(r+z)-z/r\right]; \quad (16)$$

$$d_{yz}(x,y,z)=xy^2/\left[2\pi r(y^2+z^2)\right]; \quad (17)$$

$$d_{zx}(x,y,z)=d_{yz}(y,x,z), \quad (18)$$

with $r^2=x^2+y^2+z^2$.